

Supplemental material to: Rapid transition of the hole Rashba effect from strong field dependence to saturation in semiconductor nanowires

Jun-Wei Luo,^{1,2,3,*} Shu-Shen Li,^{1,2,3} and Alex Zunger^{4,†}

¹*State key laboratory of superlattices and microstructures,
Institute of Semiconductors, Chinese Academy of Sciences, Beijing 100083, China*

²*College of Materials Science and Opto-Electronic Technology,
University of Chinese Academy of Sciences, Beijing 100049, China*

³*Synergetic Innovation Center of Quantum Information and Quantum Physics,
University of Science and Technology of China, Hefei, Anhui 230026, China*

⁴*Renewable and Sustainable Energy Institute,
University of Colorado, Boulder, Colorado 80309, USA*

* jwluo@semi.ac.cn

† Alex.Zunger@colorado.edu

Method: direct evaluation of the strength of the Rashba effect. We use our previously developed atomistic, material-dependent pseudopotential method to calculate the band structure of semiconductor nanowires under an applied electric field \mathbf{E} . The Schrödinger equation

$$\left(-\frac{1}{2}\nabla^2 + V(\mathbf{r}) + |e|\mathbf{E} \cdot \mathbf{r}\right)\psi_i(\mathbf{r}) = \epsilon_i\psi_i(\mathbf{r}) \quad (\text{S1})$$

solved within a basis set of plane waves. An energy cutoff of 5 Ry is used to select the plane-wave basis. This cutoff suffices, since it was designed at the outset in the fitting process of the pseudopotential. Fast Fourier transforms are used to transform the wave function back and forth between a real space grid and a reciprocal space grid. A $16 \times 16 \times 16$ real space grid is used for each eight-atom zinc-blende or diamond cubic cell [S1, S2]. The crystal potential $V(\mathbf{r}) = \sum_{n,\alpha} \hat{v}_\alpha(\mathbf{r} - \mathbf{R}_{n,\alpha})$ is defined by a superposition of screened atomic potentials \hat{v}_α of atom type α located at atomic site $\mathbf{R}_{n,\alpha}$,

$$V(\mathbf{r}) = \sum_{n,\alpha} \hat{v}_\alpha(\mathbf{r} - \mathbf{R}_{n,\alpha}). \quad (\text{S2})$$

The screened atomic potential \hat{v}_α contains a local part v_α^L and a nonlocal spin-orbit interaction part \hat{v}_α^{NL} . The nonlocal spin-orbit interaction \hat{v}_α^{NL} is described by a Kleinman-Bylander separable form [S2, S3]

$$\hat{v}_\alpha^{NL} = \beta_\alpha \sum_{i,j} |i\rangle B(i,j) \langle j|, \quad (\text{S3})$$

where $|i\rangle$ and $|j\rangle$ are reference functions, and $B(i,j)$ is a matrix representation of the spin-orbit interaction: $B(i,j) = \langle i|\mathbf{L} \cdot \mathbf{S}|j\rangle$, where \mathbf{L} and \mathbf{S} are the spatial angular momentum operator and spin operator, respectively. The construction of the screened pseudopotential \hat{v}_α is the key to accuracy and realism. To remove the ‘‘LDA error’’ in the bulk crystal we fit the atomic potentials \hat{v}_α to experimental transition energies, effective masses, spin-orbit splitting, and deformation potentials of the parent bulk semiconductors as described previously [S1, S2, S4]. This method is free from well-known errors of the standard density functional theory on bandgap and effective masses, and has been tested extensively over the past two decades for a broad range of spectroscopic quantities in self-assembled and colloidal nanostructures [S5], as well as been the Dresselhaus SOC effect in 3D zinc-blende semiconductors [S6], 2D quantum wells [S7], and 1D nanowires [S8]. In the atomistic approach, one does not have to commit at the outset to a linear or non-linear Rashba term, obtaining this information instead, as *output* not *input* from the quantum mechanical description of spin-orbit coupling-induced interband coupling. We do

not perform self-consistent Schrödinger-Poisson calculations because we limit ourselves to rather weak electric fields. After solving the Schrödinger equation and obtaining the energy dispersion along k_z (nanowire along z) for nanowires, the spin splitting $\Delta E_{ss}(i, k_z)$ of the band i is fit to a power series in k_z : $\Delta E_{ss}(i, k_z) = 2\alpha_R^i k_z + \gamma^i k_z^3$. The coefficients extracted from the fit determine the Rashba parameters α_R of different subbands [S9].

Dependence of the electron Rashba effect α_R on wire sizes and applied fields. Our recent work [S8] on spin splitting in zinc-blende nanowires established based on fundamental nanowire symmetry that the Dresselhaus spin splitting is absent in the (001)- and (111)-oriented nanowires with such tetrahedral bonding. An electric field applied perpendicular to the wire direction breaks the symmetry but does not evoke the Dresselhaus spin splitting, even if such spin splitting is present in 3D bulk InAs and 2D quantum wells. The field-induced spin splitting is exclusively due to the Rashba effect [S8]. Applying an electric field perpendicular to the (001)-oriented InAs zinc-blende nanowires, the obtained spin splitting is thus exclusively arising from the Rashba effect. In early reports [S10, S11], small (< 100 nm) diameter III-V nanowires showed a tendency toward forming a wurtzite phase. In recent reports, however, both pure ZB and pure WZ nanowires could be achieved across the broad range of nanowire diameters [S12–S14]. Zinc-blende InAs nanowires as small as 15 nm in diameter were routinely synthesized [S14].

In main text, Fig.1 shows atomistic calculated α_R in InAs nanowires as a function of wire radius R for a fixed electric field. Upon application of a fixed electric field $E_x = 30$ kV/cm, Fig.1 (b) exhibits that ERE α_R increases rapidly to 21.5 meVÅ up to $R = 10$ nm and begins to saturate to 34 meVÅ (a value of bulk InAs) as further increasing the nanowire diameter for InAs nanowires. The best fit of atomistic predicted α_R to model Hamiltonian formula Eq. (S6) indicates a good agreement between atomistic method and classical model Hamiltonian approach for electron Rashba effect. Fig.1 (a) shows the field-dependence of α_R for a $R = 15$ nm InAs nanowire which is linear until $E_x = 50$ kV/cm and then becomes sublinear as further increasing E_x . It clearly manifests that the Rashba effect is strongly field tunable: α_R increases from zero at the absence of electric field to as large as 136 meVÅ at $E_x = 200$ kV/cm. The slope in the linear region determines the Rashba coefficient $r_{41} = \partial\alpha_R/\partial E_x = 90.9$ eÅ², which is consistent with bulk InAs of $r_{41} = 117.1$ eÅ² [S15] with a small difference owing to quantum confinement effect, indicating the robustness of the used atomistic pseudopotential method to predict the Rashba effect.

Closed form physical model for electron Rashba α_R in nanowires. A comparison of α_R

between atomistic pseudopotential calculations and the classical model Hamiltonian approach may provide insight into the understanding of the Rashba spin splitting. The term of the Rashba effect, which originates from the spin-orbit interaction, in an effective $2 \times 2 \Gamma_{6c}$ conduction band Hamiltonian is arising from the non-commutativity of wavevector k and crystal potential V from a decoupling of conduction and valence band states [S15]. If one uses the 8×8 Kane Hamiltonian, third-order perturbation theory for the conduction band Hamiltonian yields the Rashba term [S15],

$$H_R = r_{41} \boldsymbol{\sigma} \cdot \mathbf{k} \times \mathbf{E}, \quad (\text{S4})$$

where $\mathbf{E} = (1/e)\nabla V$ is the electric field contained implicitly in the crystal potential V , here, $\mathbf{E} = (E_x, 0, 0)$ is arising from applied electric field E_x . $\boldsymbol{\sigma} = (\sigma_x, \sigma_y, \sigma_z)$ the vector of Pauli spin matrices, and a material-specific Rashba coefficient [S15],

$$r_{41} = \frac{aeP^2}{3} \left[\frac{1}{E_g^2} - \frac{1}{(E_g + \Delta_{\text{so}})^2} \right]. \quad (\text{S5})$$

Where e is electron charge, E_g the band gap of quantum structures, Δ_{so} the spin-orbit splitting ($\Delta_{\text{so}} = 0.38$ eV for bulk InAs), and P Kane's momentum matrix element ($P^2/2m = 21.5$ eV for bulk InAs). The adjustable parameter a is used to take into account all factors missed in classical Hamiltonian approach, such as (i) inter-band coupling induced by space confinement rather than by $\mathbf{k} \cdot \mathbf{p}$; (ii) Change of the quantum confinement potential induced modification of dipole matrix

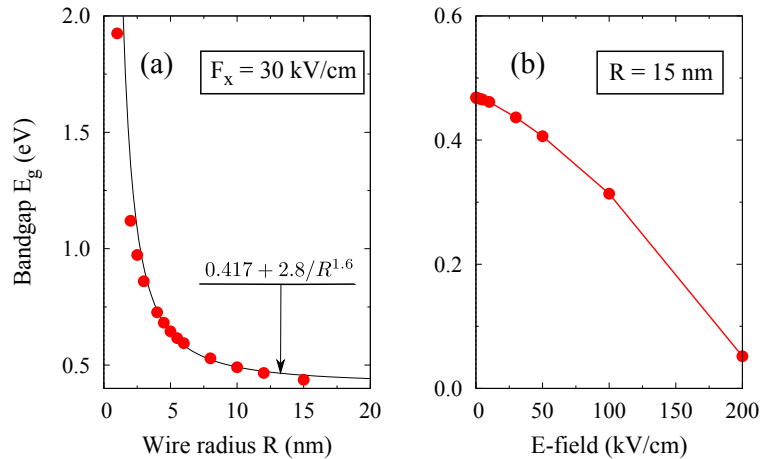


FIG. S1. (a) Atomistic method predicted bandgap E_g as a function of nanowire radius R for InAs nanowires upon application of an electric field $E_x = 30$ kV/cm. The solid line represents the best fit of the nanowire E_g . (b) Nanowire bandgap E_g as a function of electric field for the $R = 15$ nm InAs nanowire.

element P ; (iii) Energy level splitting of the valence bands; and (iv) QCSE as discussed below. The Rashba effect induced spin splitting of the conduction subband is $\Delta\epsilon(k) = 2\alpha_R k$, here the pre-factor is the named Rashba parameter,

$$\alpha_R = r_{41} E_x = \frac{aeP^2 E_x}{3} \left[\frac{1}{E_g^2} - \frac{1}{(E_g + \Delta_{so})^2} \right]. \quad (\text{S6})$$

The value of a could be inferred by fitting atomistic predicted α_R to Eq. (S6). In doing so, we first describe atomistic predicted $E_g(R)$ of InAs nanowires with radius R by a formula $E_g(R) = E_g^b + \beta/R^\gamma$ as shown in Fig. S1(a), here $E_g^b = 0.417$ eV is bulk InAs band gap [S16], and $\beta = 2.8$ and $\gamma = 1.6$ for InAs nanowires under $E_x = 30$ kV/cm. Taking a as the only adjustable parameter, we subsequently fit atomistic predicted $\alpha_R(R)$ to Eq. (S6), shown in Fig. 2 (a). Our best fit indicates $a = 0.92$. This value is close to $a = 0.96$ for the rectangular well and $a = 1$ for the parabolic well [S15], with an infinite energy barrier [S15], implying that the contributions from missed four factors to α_R are small, at least for nanowires under a moderate electric field of $E_x = 30$ kV/cm.

[S1] L.-W. Wang and A. Zunger, Physical Review B **51**, 17398 (1995).

[S2] L.-W. Wang, J. Kim, and A. Zunger, Physical Review B **59**, 5678 (1999).

[S3] L. Kleinman and D. M. Bylander, Physical Review Letters **48**, 1425 (1982).

[S4] A. J. Williamson, L. W. Wang, and A. Zunger, Phys. Rev. B **62**, 12963 (2000).

[S5] G. Bester and A. Zunger, Phys. Rev. B **72**, 165334 (2005).

[S6] J.-W. Luo, G. Bester, and A. Zunger, Physical Review Letters **102**, 056405 (2009).

[S7] J.-W. Luo, A. N. Chantis, M. van Schilfgaarde, G. Bester, and A. Zunger, Physical Review Letters **104**, 066405 (2010).

[S8] J.-W. Luo, L. Zhang, and A. Zunger, Physical Review B **84**, 121303 (2011).

[S9] Since the Dresselhaus effect for 1D nanowires made of zinc-blende semiconductors vanishes by symmetry [S8] for the (001)- and (111)-directions, any spin splitting we find upon application of an electric field perpendicular to the nanowire is fully a consequence of the Rashba effect arising from the breaking of the structural inversion symmetry.

[S10] F. Glas, J.-C. Harmand, and G. Patriarche, Physical Review Letters **99** (2007), 10.1103/PhysRevLett.99.146101.

- [S11] J. Johansson, K. A. Dick, P. Caroff, M. E. Messing, J. Bolinsson, K. Deppert, and L. Samuelson, *The Journal of Physical Chemistry C* **114**, 3837 (2010).
- [S12] H. J. Joyce, J. Wong-Leung, Q. Gao, H. H. Tan, and C. Jagadish, *Nano Letters* **10**, 908 (2010).
- [S13] Y. Zhao, X. Li, W. Wang, B. Zhou, H. Duan, T. Shi, X. Zeng, L. Ning, and Y. Wang, *Journal of Semiconductors* **35**, 093002 (2014).
- [S14] M. Fu, Z. Tang, X. Li, Z. Ning, D. Pan, J. Zhao, X. Wei, and Q. Chen, *Nano Letters* **16**, 2478 (2016).
- [S15] R. Winkler, *Spin-orbit coupling effects in two-dimensional electron and hole systems*, Springer tracts in modern physics No. v. 191 (Springer, Berlin; New York, 2003).
- [S16] I. Vurgaftman, J. R. Meyer, and L. R. Ram-Mohan, *Journal of Applied Physics* **89**, 5815 (2001).